

Search for resonance rings in disk galaxies at $0.1 < z < 0.9$

Z. Karamat,¹ and K. Bekki,²

¹ *ICRAR M468 The University of Western Australia 35 Stirling Hwy, Crawley Western Australia 6009, Australia*

² *ICRAR M468 The University of Western Australia 35 Stirling Hwy, Crawley Western Australia 6009, Australia*
Australia

28 November 2022

ABSTRACT

Although the redshift evolution of the number fraction of barred galaxies has been extensively investigated so far, such z evolution for disk galaxies with resonance rings has not been investigated so much. Here we investigate the number fraction of spiral galaxies with outer rings possibly formed through dynamical action of bars at different redshifts using $\sim 75,000$ images of spiral galaxies from the second data release of the Hyper Suprime-Cam Subaru Strategic Program (HSC SSP). Since the number of galaxies to be classified is very large, we use the convolutional neural networks (CNNs) to classify spiral galaxies into those with or without outer rings. The principal results are as follows. (1) evolution of number fraction of ring with respect to photometric and spectroscopic redshift, (2) evolution of number fraction of barred ring with respect to photometric and spectroscopic redshift, (3) Investigation of physical properties of galaxies at intermediate and high z and comparison of physical properties of ring and non ring galaxies.

Key words: galaxies: star clusters – early-type galaxies: general – stars: formation

1 INTRODUCTION

Stellar and gaseous rings within and around galaxies can have valuable information on their formation and evolution histories (e.g., Buta & Combes 1996). These rings can be classified into the three categories (Buta 2000), (i) “resonance rings” formed from dynamical interaction between stellar bars and disks, (ii) collisional rings in interacting and merging galaxies (e.g., Appleton & Struck-Marcell 1996), and (iii) polar rings preferentially found in S0s (e.g., Whitmore et al. 1990). Numerical simulations have shown that the formation processes of these rings are quite different and reflected on the detailed physical properties of the rings (e.g., Bekki 1998). The outer resonance rings are particularly important in discussing the long-term dynamical evolution of barred disk galaxies through dynamical action of the stellar bars on field stars within the disks.

Although the physical properties of nearby ring galaxies have been investigated in detail, those of ring galaxies at intermediate and high z have not been done so (e.g., Buta 2000). If the outer resonance rings in disk galaxies can be formed as a result of secular evolution of stellar bars within the disks, it is possible that the fraction of disk galaxies with resonance rings (f_r) can be smaller at higher z : galaxies just after bar formation should not have outer resonance rings. Given that there are a number of existing studies on the number fraction of barred galaxies (f_{bar}), if z evolution of

f_r (if combined with f_{bar} evolution) is newly revealed for a statistically enough number of disk galaxies, then such an observational results can possibly provide crucial information on the secular evolution of disk galaxies driven by stellar bars.

A large number ($\sim 70,000$) of galaxy images from the second public release of the Hyper Suprime-Cam Subaru Strategic Program (HSC SSP) should be very useful for discussing the z evolution of f_r , because there is an enough number of disk galaxies (> 1000) for each redshift bin. Furthermore, recent observational studies based on the HSC data have already derived a number of global properties of the galaxies such as the shapes of spiral arms, bulge mass fractions, and total stellar masses (e.g., Tadaki et al. 2019), which can be used to investigate the correlations between the physical properties of rings and those of other properties. The presence or absence of stellar bars in these images have been also investigated, which make it possible for the present study to investigate the ring properties in barred and non-barred disk galaxies.

Although such a classification tasks is very important for better understanding the origin of ring galaxies, it is time-consuming for astronomers, in particular, when a large number ($> 10,000$) of disk galaxies should be classified by human eyes (manually). Recently, convolutional neural networks (CNNs) have been used to automate morphological classification tasks. Convolution neural networks have the

ability to perform complex classification task by detecting important features without the need of human supervision. Once the model is trained it can categorize huge amount of two dimensional images of galaxies automatically based on visual feature, saving a lot of time.

The purpose of this paper is to try to find possible candidates of outer stellar rings in disk galaxies at intermediate and high z through new applications of CNNs to galaxy images from the HSC SSP. To do so, we first train our CNNs using a large number of existing galaxy images with or without outer rings (“labels” in supervised learning). We then apply the trained CNNs to the HSC data set to select very good candidates of disk galaxies with outer rings. For these selected candidates, we investigate the physical properties of the galaxies such as the bulge mass fractions, photometric and spectroscopic redshifts (z_{photo} and z_{spectro} , respectively), and stellar disk masses (M_s). We particularly investigate the redshift evolution of (i) the number fraction of ring galaxies (f_r) and (ii) that of barred galaxies with rings.

The plan of the paper is as follows. We describe the details of our new method based on deep learning to classify disk galaxies into those with or without rings in §2. In this section, we briefly describe the image data sets from the DR2 of HSC-SPP. We present (i) the physical properties of the selected rings in barred and non-barred galaxies and (ii) key results of z evolution of f_r in §3. We provide several implications of these results on the cosmological evolution of f_r in disk galaxies in §4. We summarize our conclusions in §5.

2 THE MODEL

2.1 Overview of a method to classify galaxies

In order to classify the ring and no ring galaxy images. A CNN was trained on catalog by Nair & Abraham (2010). It contained 14000 images of galaxies with 1207 ring galaxies and 12827 no ring galaxies. The CNN model trained on Nair & Abraham (2010) was used to classify ring and no ring galaxies in Tadaki dataset. Fig.1 shows the images of spiral galaxies with and without ring from Tadaki dataset. Fig.2 shows the confusion matrix for CNN model. The galaxies classified by the CNN model were not very accurately classified into the target classes. The images classified by the CNN model were cleaned manually to pick only accurate ring images as shown in Fig.3. This cleaned data set was then combined with Nair & Abraham (2010) to train the CNN. There also existed class imbalance problem so data augmentation technique was used to increase the samples in minority class. The classification results produced by the CNN trained on combined cleaned data were accurate as compared to previous results. Fig.3 shows the ring galaxies accurately classified by the CNN while Fig.4 shows non ring galaxies as a result of CNN classification.

2.2 Training CNNs with real images of galaxies

Initially resnet-18 model was trained on Nair & Abraham (2010). Resnet-18 is an 18 layered Convolution Neural Network. 20% of data is chosen as validation set. Each is resized

z_{photo}	N	N_r	N_{nr}	$N_{r,b}$	$N_{r,nb}$	f_r
0 - 0.1	4343	1559	2784	1038	521	0.358
0.1-0.2	23716	6460	17256	4220	2240	0.272
0.2-0.3	22614	4286	18328	2754	1532	0.189
0.3-0.4	17476	2410	15066	1677	733	0.137
0.4-0.5	5446	826	4620	510	316	0.151
0.5-0.6	1750	256	1494	178	78	0.146
0.6-0.7	774	81	693	50	31	0.104
0.7-0.8	69	9	60	5	4	0.130
0.8-0.9	27	3	24	2	1	0.111

Table 1. The table shows the number of galaxy images(N), ring galaxies(N_r), barred ring galaxies($N_{r,b}$), non barred ring galaxies($N_{r,nb}$) and ring fraction(f_r) with respect to photometric redshift (z_{photo})

to (64X64) and normalized. Images are augmented by Horizontal and Vertical flips, and random rotation with $\pm 10^\circ$. Due to the complexity of model, it could not generalize the data so it overfitted the data. To overcome this problem a less complex model Alexnet was used. Alexnet has only 5 convolutional layers followed by filters and 3 fully connected layers for classifications. Adam optimizer along with cross entropy loss was used to optimize the model. The learning rate initially was set 0.0001 and was decayed after every 7 epochs. The model was trained for 50 epochs. The validation accuracy for the model was 89% compared to 74% by resnet model .

2.3 HSC SPP data

KB will write this.

2.4 Evolution of ring galaxy fraction

We mainly investigate how the number fraction of spiral galaxies with outer resonance rings evolve with z using $\sim 77,000$ spiral galaxy samples. The fraction of ring galaxies is defined as follows;

$$f_r = \frac{N_r}{N}, \quad (1)$$

where N and N_r are the total number of spiral galaxies and that of spirals with outer rings, respectively. The number of spirals without rings is defined as N_{nr} . For each z range (e.g., 0.1 – 0.2), we investigate N and N_r using the results of CNN-based classification and photometric and spectroscopic redshifts (z_{photo} and z_{spect} , respectively) in the original catalogue by Tadaki et al. (2020, T20).

We also investigate the redshift evolution of the number fraction of spirals with both rings and bars in order to understand better the formation processes of resonance rings through dynamical action of stellar bars in stellar disks. We use the results in our recent paper (Nguyen & Bekki 2021) in which spiral galaxies in T20 are classified into barred or non-barred (two-way classification). The number fraction of spirals with both rings and bars ($f_{r,b}$) is defined as follows;

$$f_{r,b} = \frac{N_{r,b}}{N_r}, \quad (2)$$

where $N_{r,b}$ is the total number of spiral galaxies with both outer rings and bars. The number of spirals with rings yet without bars is defined as $N_{r,nb}$.

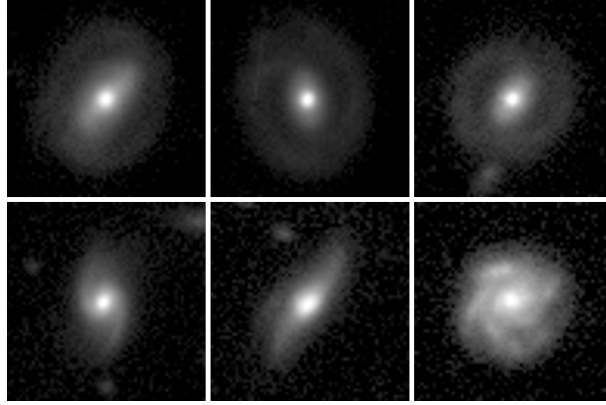


Figure 1. A montage representing ring and no ring galaxy images used in training CNN. Top columns show images of ring galaxy with rings that could be seen clearly. Bottom column shows non ring galaxy images.

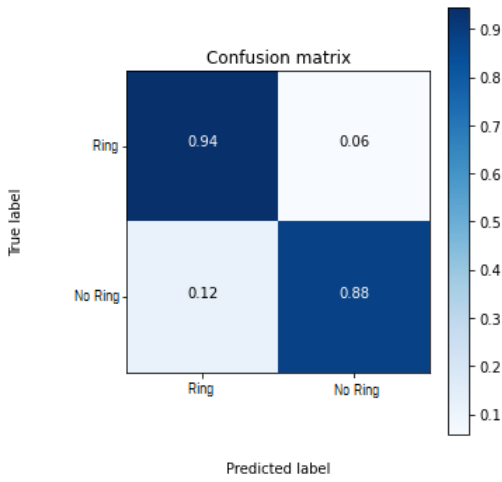


Figure 2. Confusion matrix for the classification of 75000 HSC disk galaxies with or without rings by CNN model

	f_{bul}	$\log M_{\odot}$	$SFR (M_{\odot}/yr)$
Ring	-0.0871051	10.464	0.0580415
No Ring	-0.345551	10.1734	0.262075

Table 2. The table shows the mean value of f_{bul} (fraction of flux in de Vaucouleur component), stellar mass and SFR (star formation rate) among ring and non ring galaxies.

3 RESULTS

3.1 Morphological properties of the selected rings

3.2 z evolution of the number fraction of spirals with rings

The overall pattern of evolution of number fraction of spiral having rings (f_r) is decreasing with the increasing photometric (z_{photo}) as well as spectroscopic redshifts (z_{spect}). However the fraction slightly increases as z_{photo} changes from 0.3 to 0.5. The results of evolution of number fraction for ring galaxies is illustrated in Table 1 for each bin of z_{photo} .

3.3 Physical properties of rings

The study compares the physical properties of ring galaxies with non ring galaxies as shown in Table 2. It has been found out that mean fraction of flux in de Vaucouleur profile f_{bul} is around -0.0871 which is higher than non ring galaxies. The star formation rate SFR of ring galaxies is lower than the non ring galaxies having mean value of 0.05804. Whereas the stellar mass for both ring and non ring galaxies is close to each other with the mean value of 10.464 for ring galaxies.

4 DISCUSSION

4.1 Comparison with the observed z -evolution of barred galaxies

KB will write this.

4.2 z -evolution of other types of rings

KB will write this.

5 CONCLUSIONS

We have used the new image data from the HSC SPP project in order to discover spiral galaxies with outer rings (“resonance rings”) possibly formed from dynamical action of stellar bars within the disks. First we have trained CNNs using a subset of these images and applied the CNNs to the rest of 70,000 images to find resonance rings. In the present study, we have used ResNet to classify spiral galaxies into the two categories, i.e., spirals with or without outer rings, after we have revised ResNet slightly. We have investigated the physical properties of spirals with or without rings, in particular, the redshift evolution of the number fraction of spirals with rings (f_r). The main results are as follows:

please list up several key results and describe them here like below;

(1) Our CNN can properly classify galaxies into spirals with or without rings with an accuracy of 89%. This level of prediction accuracy is not so ideal (i.e., not very close to 100) we consider that our CNN can be still used to discuss the

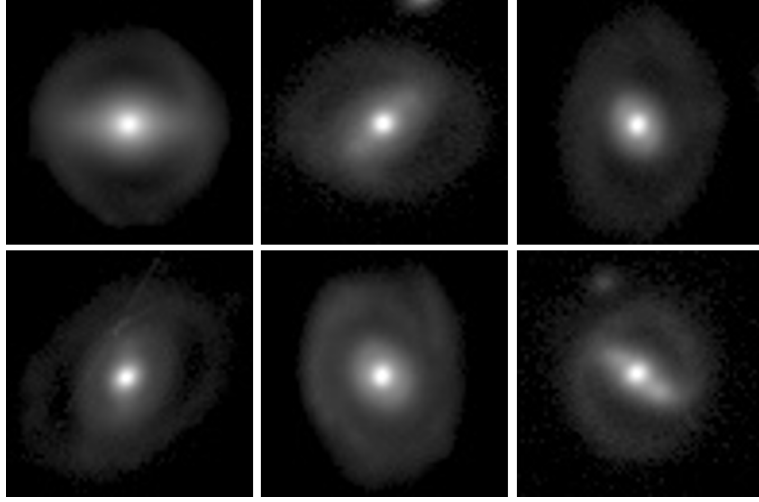


Figure 3. The same as Fig. 1 but ring galaxy images classified by the CNN model

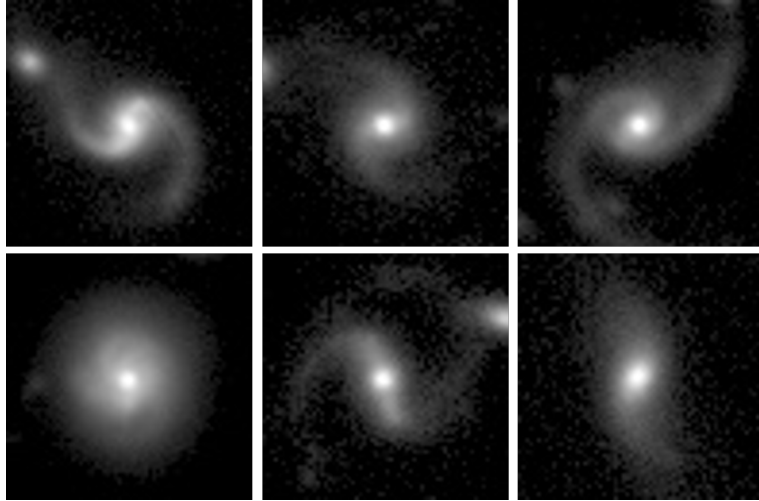


Figure 4. The same as Fig. 1 but non ring galaxy images classified by the CNN model

statistical properties of ringed galaxy populations at different redshifts. The major reason for this miss-classification is that some ring galaxies are very hard to distinguish even with the naked eye. Also some images contain galaxies that are very small in size. Improving the quality of images used in training could improve the accuracy of model.

(2) The number fraction of spiral galaxies with outer rings decreases with increasing z (i.e., smaller fraction in higher z), though the photometric redshifts (z_{photo}) are used in the present study.

The galaxies with $z_{photo}=0.1$ have a f_r 0.358. f_r decreases as z_{photo} is increased, eventually f_r drops to 0.111 for $z_{photo}=0.9$. The same pattern is followed for z_{spect} where f_r is 0.1987 for $z_{spect} = 0.2$ and f_r drops to 0.096 for $z_{spect} = 0.8$. Table 1 gives the detailed information about the fractions for each photometric z_{photo} redshift bin. Fig. 5 illustrates the results of decreasing fraction f_r for photometric z_{photo} and spectroscopic z_{photo} . In this Fig. 5, the f_r on y-axis represent the ring fraction whereas z_{photo} and z_{spect} on x-axis represent the bins for photometric and spectroscopic

redshifts. The error bar represents mean square root errors in each redshift bin.

(3) About 66 % of spirals with rings have stellar bars. The fraction(f_{rb}) of spiral with both rings and bars also show the same decreasing pattern as followed in ring galaxies. Fig. 7 clearly demonstrates the decreasing fraction f_{rb} on y-axis over increasing photometric z_{photo} and spectroscopic z_{spect} redshifts on x-axis. The error bar represents mean square root errors in each redshift bin. f_{rb} is 0.239 for $z_{photo}=0.1$ and 0.130 for $z_{spect}=0.2$. This fraction drops to 0.0724 for $z_{photo}=0.9$ whereas 0.0564 for $z_{spect}=0.8$

(4) Ring and Non ring galaxies also show a difference in the other physical properties such as stellar mass, star formation rate and the fraction of flux in de Vacucouleux component. Table 2 illustrates the values for these physical properties among ring and non ring galaxies **Other results to be added by Zeeshan.**

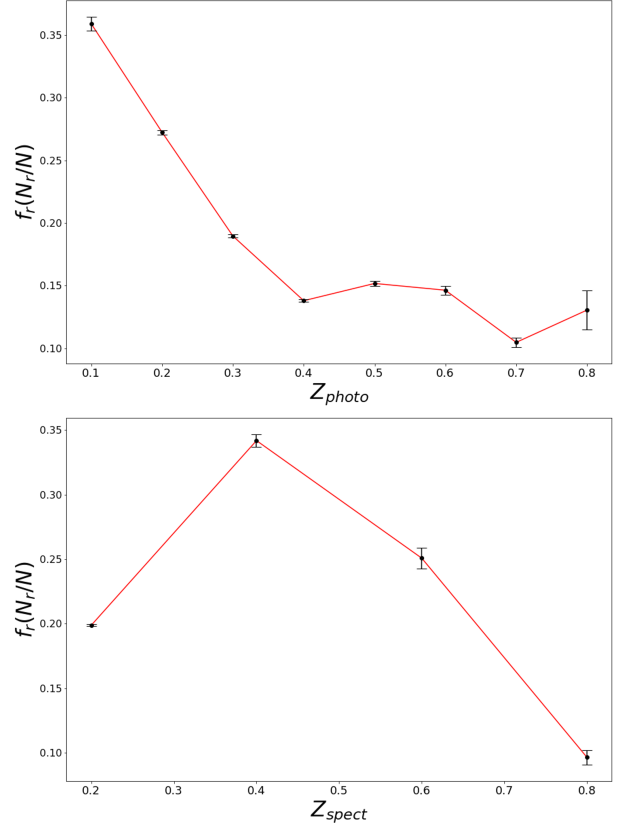


Figure 5. The figure shows the comparison of redshift evolution of ring fraction with respect to photometric (z_{photo}) and spectroscopic (z_{spect}) redshift

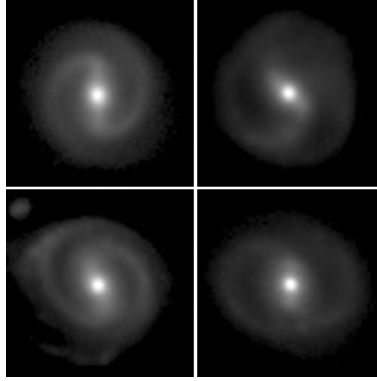


Figure 6. Shows the images of barred galaxies among ring galaxies.

REFERENCES

Agnew, D. C., Earth Tides, In: Herring, T. ed. *Geodesy: Treatise on Geophysics*, Elsevier, 163–197, 2010.

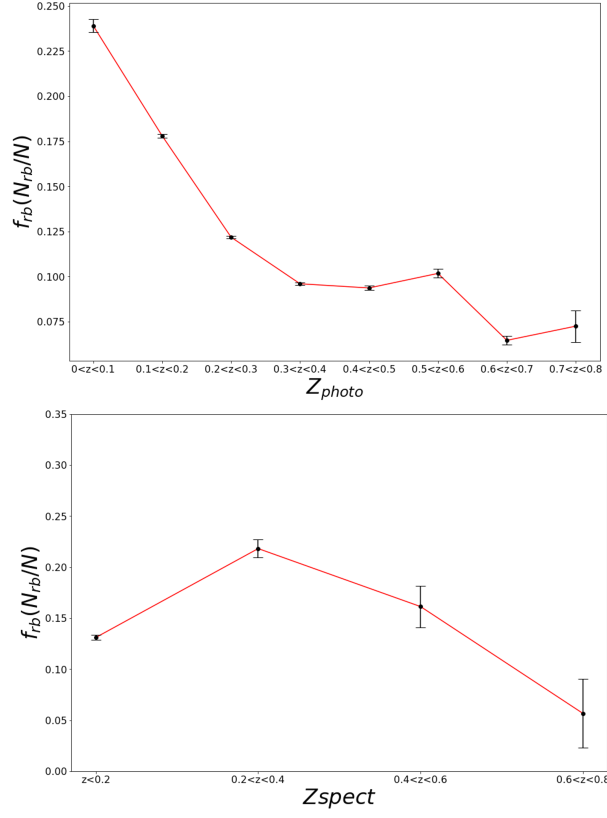


Figure 7. The figure shows the comparison of redshift evolution of barred galaxy fraction with respect to photometric (z_{photo}) and spectroscopic (z_{spect}) redshift.

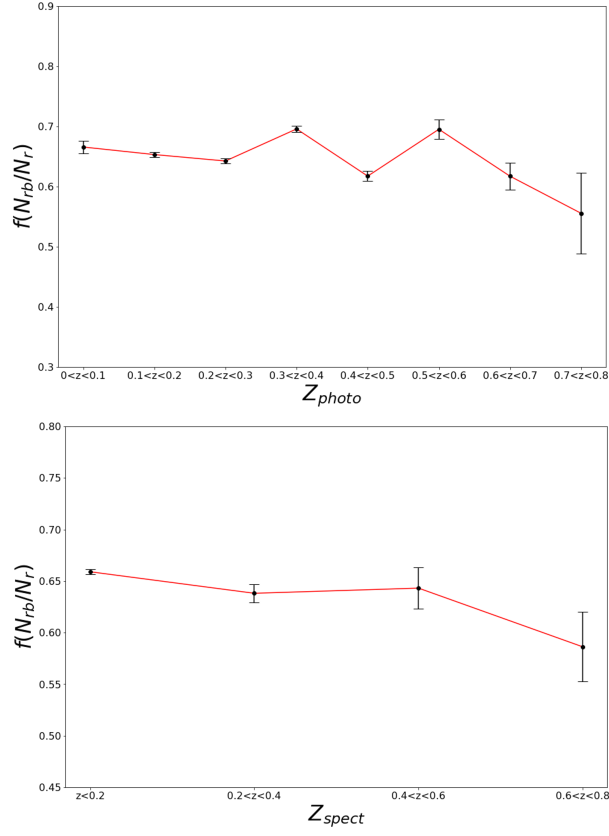


Figure 8. The figure shows the comparison of redshift evolution of barred galaxy fraction among ring galaxies with respect to photometric (z_{photo}) and spectroscopic (z_{spect}) redshift.

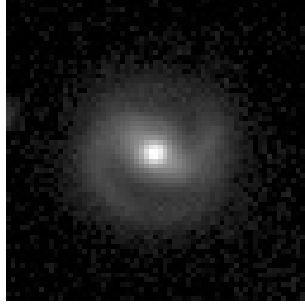


Figure 9. The most distant galaxy with respect to spectroscopic redshift among ring galaxy images having $z_{spect} = 0.5986$

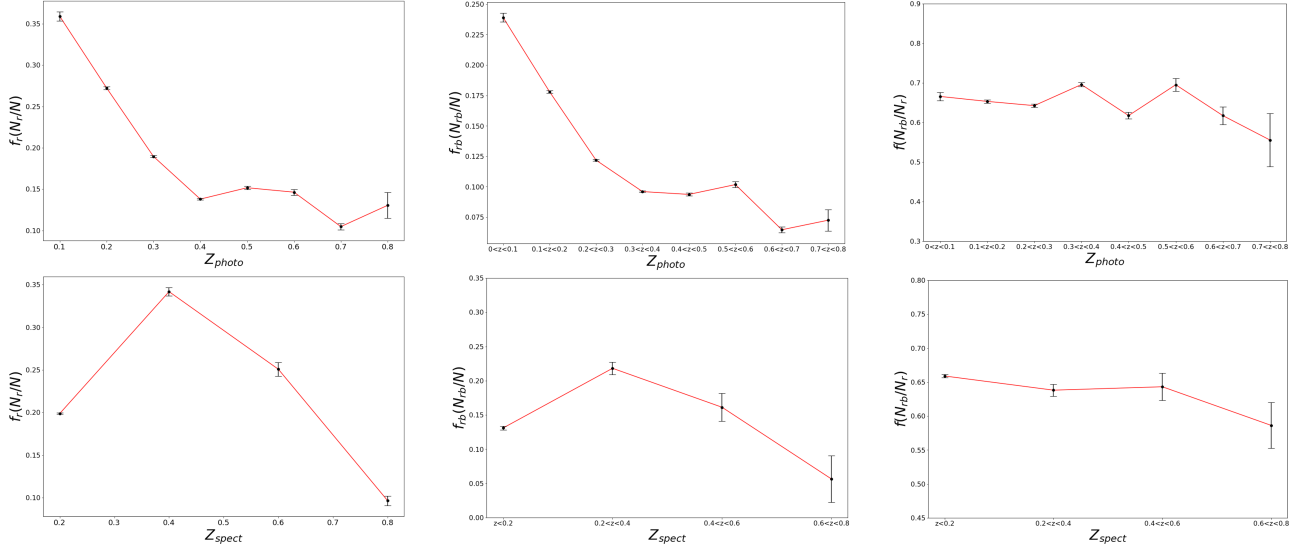


Figure 10. Grouped photo for fig5,fig7,fig8